# Building IoT-Enabled Wearable Medical Devices: An Application to a Wearable, Multiparametric, Cardiorespiratory Sensor

Arthur Gatouillat[1], Bertrand Massot[2], Youakim Badr[1], Ervin Sejdić[3] and Claudine Gehin[2]
[1]*Univ. Lyon, INSA-Lyon, LIRIS, UMR5205, F-69621, France*
[2]*Univ. Lyon, INSA Lyon, INL, UMR5270, F-69621, France*
[3]*Department of Electrical and Computer Engineering, Swanson School of Engineering, University of Pittsburgh, Pittsburgh, PA, U.S.A.*

Keywords: Wearable Sensor, Medical IoT, Heart Rate Sensor.

Abstract: Recent developments in personal and mobile healthcare have shown promising results in term of patients' quality of life and quality of care improvements. This can be achieved through continuous monitoring of patients' physiological functions using wearable non-invasive biomedical sensors. The remote collection and processing of such data can then be used to provide rapid medical response if a problem is detected or to offer preventive measures. However, the integration of wearable sensors into wider-scale framework is still a major challenge, as real-time data collection and remote configuration capabilities must be integrated to strongly constrained devices. Here, we show how such requirements can be integrated into a multiparameter, cardiorespiratory wearable sensor and how this sensor can be integrated into wide-scale Internet-based frameworks. We thus manufactured a biomedical-grade heart rate, instantaneous heart-rate variability and respiratory sensor. The sensor was tested in real life ambulatory condition, and we showed an Internet-based proof of concept exhibiting the integration of our sensor into wide-scale healthcare frameworks. Finally, we anticipate that wearable healthcare will greatly improve patients' quality-of-life by using IoT-based wearable devices similar to the sensor developed in this paper.



## 1 INTRODUCTION

Personalized and mobile healthcare are growing fields of interest in the biomedical community. The idea behind such concepts is to provide patients with health recommendations and diagnostic tailored to their individual needs. This can be achieved using continuous remote monitoring of the patients' physiological functions associated with data analysis to offer preventive measures, or rapid medical response if a physiological malfunction is detected. Consequently, personalized healthcare is a promising approach to improve the financial and therapeutic efficiency of healthcare (Van Hoof and Penders, 2013), by avoiding unnecessary hospitalization while preserving the safety of the patients.

Personalized healthcare can be achieved using wearable sensors networks (Massot et al., 2013), which are used to accurately monitor vital signs. Cardiac health estimation devices are of particular interest because of the crucial nature of the cardiac function and because it has been well explored by the biomedical sensor community, for instance in (Massot et al., 2015), (Magno et al., 2014), (Altini et al., 2011), (Khayatzadeh et al., 2013) and (Tuominen et al., 2017). Moreover, cardiac activity parameters can be used as an indicator of several pathologies. In particular, heart rate variability (HRV) provides insights about the autonomic nervous system parameters which reflects the patients' emotional state (Task Force of the European Society of Cardiology the North American Society of Pacing Electrophysiology, 1996). However, one of the major research problem at the moment is the integration of developed wearable sensors into bigger frameworks. Indeed, personalized healthcare assumes health data to be collected in real-time and that such data is analyzed by powerful algorithms on distant servers. Personalized healthcare also makes remote sensor reconfiguration necessary in order to better suit both patients and healthcare professional expectations.

All the identified wearable electrocardiogram-based cardiac activity sensors, despite accurately measuring cardiac activity parameters, do no feature enough connectivity and functionality to be able to



Gatouillat, A., Massot, B., Badr, Y., Sejdić, E. and Gehin, C.
Building IoT-Enabled Wearable Medical Devices: An Application to a Wearable, Multiparametric, Cardiorespiratory Sensor.
DOI: 10.5220/0006729101090118
In *Proceedings of the 11th International Joint Conference on Biomedical Engineering Systems and Technologies (BIOSTEC 2018) - Volume 1: BIODEVICES*, pages 109-118
ISBN: 978-989-758-277-6

use them in a personalized healthcare context. Only wearable ECG or ECG-based cardiac parameters sensors were studied because of their accuracy in terms of cardiac parameters estimation. Although widely used, the accuracy of other popular methods such as plethysmography is still questioned by the community (Schäfer and Vagedes, 2013) and suffer from heavy movement artifact. Authors of (Magno et al., 2014) designed a wearable heart rate and respiratory rate sensor with Bluetooth low energy and proprietary 802.15.4 connectivity by combining several development kits. This solution lacks remote configuration capabilities and proper integration, which both are critical aspects of personalized healthcare. In (Tuominen et al., 2017), a remotely configurable ECG sensor was designed, but data is stored locally on a SD card, which makes this solution unsuitable for remote healthcare applications. Another wearable ECG sensor was developed by (Izumi et al., 2015), is remotely configurable, and data are sent using wireless connectivity. However, this device use near field communication (NFC) for all of its connectivity. The short range of NFC application makes it unpractical for real life data collection, as data can only be collected when a NFC reader is brought in proximity of the sensor. A heart rate (HR) and HRV sensor is described in (Massot et al., 2015). This device offers on-board cardiac parameters calculation, and computed parameters are sent to a smartphone using wireless connectivity. However, this sensor is not remotely configurable, and data is only stored locally on the smartphone, which makes some adaptation necessary in order for this device to be used in a personalized healthcare concept.

Recently, the study of the interconnection of multiple devices featuring real-time data collection and remote configuration capabilities was studied under the scope of the Internet-of-Things (IoT) (Gubbi et al., 2013). In the IoT, a variety of heterogeneous communicating devices are interconnected, but also communicate with external services implemented on remote servers. Consequently, the IoT seems like an approach of particular interest when trying to solve the challenges of wide-scale personalized healthcare (Fernandez and Pallis, 2014), and this paper will describe the integration of IoT characteristics on a biomedical wearable cardiac and respiratory sensor to enable its integration into a wide scale personalized healthcare framework.

Our solution focuses on the integration of remote reconfiguration capabilities to our sensor, the implementation of different functional modes to enable adaptive capabilities, and the real-time streaming of biomedical data. All these functionalities must preserve measurements accuracy. The impact of integrating IoT characteristics to the sensor on both hardware and software designs, but also on the overall consumption of the device was carefully studied in order to ensure our sensor validity from a real-life perspective.

The following paper is organized as follows. Section 2 introduces the materials and methods enabling the integration on IoT properties to a biomedical grade sensor, but also describes the design of analog/digital electronics to achieve the desired functional and non-functional goals. In section 3, we present a comprehensive caracterization of the sensor from a power consumption and data quality evaluation perspective, and finally section 4 discusses the potential application of such sensor for patients and medical practitioners.

## 2 MATERIALS AND METHODS

The manufactured IoT-enabled wearable cardiac and respiratory activity sensor is displayed in Figure 1.a. This circuit board is small (40 mm $\times$ 20 mm $\times$ 6 mm), and it is packaged along with a 300 mAh battery in a plastic enclosure. The complete sensor (i.e., PCB, battery, plastic enclosure and cables) weighs only 26.7 g, making it light enough for wearable applications.The sensor is designed to be used with three electrodes: left arm, right arm and a common mode rejection electrode, as illustrated in Figure 1.b. The left arm and right arm electrodes are connected to the sensor using wires, and the sensor is directly attached to the common mode rejection electrode. Consequently, the device can be comfortably worn by the patients for extended periods of time. The battery of the sensor is charged using the micro-USB port, and the sensor can be reset to its default state using the single push-button of the device. This sensor is able to measure both the heart rate, heart rate variability parameters and the respiration waveform (RWF).

### 2.1 Sensor Hardware Description

The global sensor architecture is given in Figure 2. Because of the potential overhead due to the addition of IoT-related characteristic to our device, components were selected in order to maximize their computational and power efficiency.

In order to minimize CPU load and CPU wake-up time caused by real-time signal processing, it must be performed using dedicated hardware. This led to the choice of a PSoC 5LP (Cypress Semiconductor, San Jose, CA) for the device microcontroller and dedicated signal processor. Indeed, this integrated circuit (IC) offers both an ARM Cortex Core M3 CPU

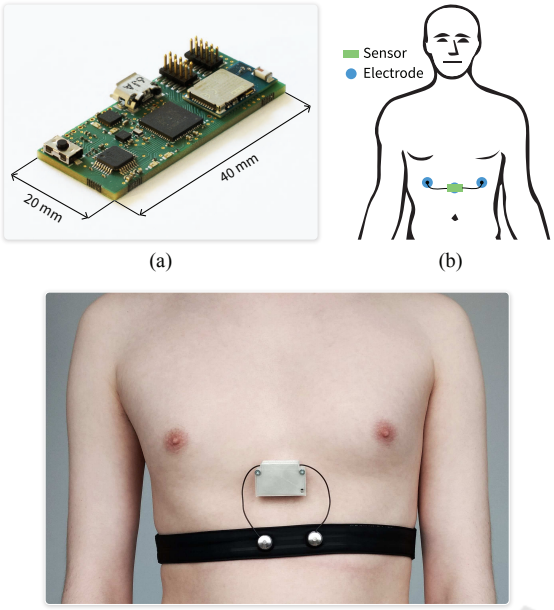


(a) (b)

(c)

Figure 1: Manufactured sensor (a), body placement (b) and sensor worn in ambulatory conditions (c).

core and a programmable digital filter block in a single package, leading to smaller PCB, thus improving the comfort of the patients. Because Bluetooth Low Energy (BLE) is the main protocol used in resource constrained devices for the IoT and because of its widespread adoption (Harris III et al., 2016), it was selected to provide wireless connectivity to our sensor. The BLE113 integrated chip (Silicon Labs, Austin, TX) was selected as the BLE dedicated microprocessor because it integrates both a full hardware and software BLE stack with integrated antenna design in a small 15.75 mm $\times$ 9.15 mm $\times$ 1.9 mm package. This integrated circuit is fully programmable, and all communication dedicated firmware can be deployed on this IC, thus reducing the microprocessor computing load. In order to be able to simultaneously measure both the ECG and the respiration waveform, the ADS1292R (Texas Instruments, Dallas, TX) was selected. This low-power analog front-end (AFE) integrates two differential amplifiers and two 24 bits analog to digital converters. It also features a right-leg drive (RLD) amplifier to implement common mode rejection (Winter and Webster, 1983) along with lead-off and respiration signal modulation and demodulation circuitry. The measurements are sent using a SPI bus at a configurable sampling rate (from 125 to 8000 samples per seconds).

In the default state, the analog front end is configured to measure both the respiration waveform on channel 1 and the ECG signal on channel 2 at a sampling rate of a 1000 SPS using the internal clock of the IC. This sampling rate enables a 1 ms resolution for RR interval measurements. The RLD amplifier and lead-off detection circuitry are both enabled, along with the respiration modulation and demodulation modules.

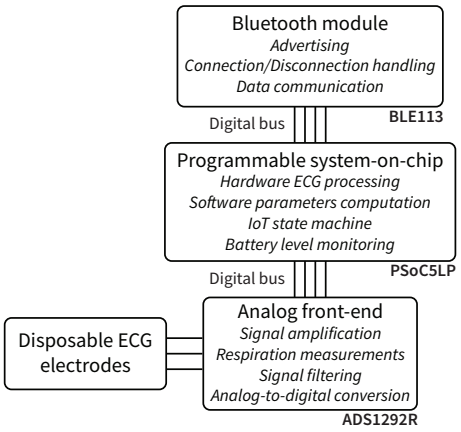


Figure 2: Hardware architecture of the sensor.

The RR interval computation is implemented using hardware filtering and peak detection. The digital filter block of the PSoC5LP is used to compute the smoothed moving average derivative of the ECG signal, which is then used in combination with adaptive thresholding in order to compute the RR interval. Details about the implementation are given in Figure 3 and in (Massot et al., 2016).

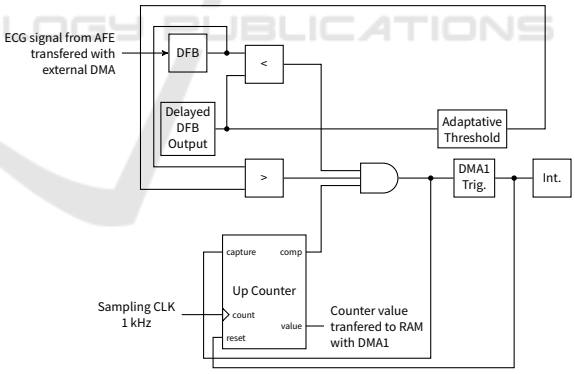


Figure 3: Hardware detection of RR intervals.

Using this hardware-centric approach to perform computationally intensive real-time signal processing reduces the CPU load and increases the CPU sleep time, thus reducing global power consumption. All the other sensor functional tasks are implemented using a software approach, and will thus be further described in the following section.

## 2.2 Sensor Software Description

The firmware of the sensor was developed to achieve several functional and non-functional goals. The first goal is focused on the measurements and their transmission: the real-time communication of the instantaneous heart rate, the computation and communication of HRV parameters every 5 minutes, the real-time communication of 6 respiration samples every second. The second goal is to transmit non-functional information about the sensor, typically the battery level or if the sensor is unattached. Finally, the last goal is the implementation of IoT dedicated software, which is used to integrate the sensor into a wider IoT-based framework. Such software is used to transmit information about the sensor state in order to trigger remote sensor configuration.

### 2.2.1 Measurements Dedicated Software

This firmware is implemented on the PSoC5LP, and it can be divided into three sections: the computation of the instantaneous heart rate when a heart beat is detected (i.e., when an interruption is triggered by the peak detection hardware). The heart rate can be easily computed using the following equation:

$$HR_{\text{BPM}} = \frac{60 \times SR}{RR_{\text{int.}}} = \frac{60 \times 1000}{RR_{\text{int.}}} \quad (1)$$

where $HR_{\text{BPM}}$ is the instantaneous heart rate in beats per minutes (BPM), $SR$ is the sampling rate in samples per seconds and $RR_{\text{int.}}$ is the RR interval in samples. This computation is implemented directly on the microcontroller and the RR interval values are buffered to be used in the HRV parameters computation.

Every 5 minutes, the HRV parameters are computed from the buffered RR interval values in accordance with the recommendations of the joint Task Force of the European Society of Cardiology (Task Force of the European Society of Cardiology the North American Society of Pacing Electrophysiology, 1996), and these parameters are summarized in Table 1.

The computation of the frequency domain parameters are based on the power spectral density (PSD) estimation. Because the RR intervals signal is unevenly sampled, the Lomb-Scargle periodogram (Lomb, 1976) was determined using the fast computation algorithm developed by (Press and Rybicki, 1989). We used the same optimal algorithmic parameters than (Massot et al., 2016). Indeed, authors of (Massot et al., 2016) conducted a systematic evaluation of the impact of the parameters on the trade-off between computation time and periodogram precision, resulting in the proposition of optimal parameters with respect to both the periodogram precision and the computation time.

Table 1: Computed HRV parameters

| Variable | Unit | Domain | Description |
|---|---|---|---|
| SSDN | ms | Time | Standard deviation of buffered RR intervals |
| RMSSD | ms | Time | Quadratic mean of differences between consecutive RR intervals |
| LF/HF | n.u. | Freq. | Low-frequency (0.04 to 0.15 Hz) to high-frequency (0.15 to 0.4 Hz) components ratio of the PSD of the buffered intervals |
| Norm. LF | % | Freq. | Normalized low-frequency components to sum of low- and high-frequency components of the PSD ration, i.e., LF/(LF+HF) |

The respiration waveform is buffered in the RAM of the PSoC5LP, and is transmitted wirelessly every second. The first step of the respiration signal processing is the downsampling of the respiration signal from 1000 SPS to 6 SPS. A sampling frequency of 6 Hz, resulting in a Nyquist rate of 3 Hz, is well within the bandwidth of respiratory signals, which is at most 1.5 Hz (Zhao et al., 1994), and decreasing the sampling rate reduces energy consumption because of the smaller amount of transmitted information. After signal downsampling, the respiration waveform is smoothed using an exponential filter:

$$y[n] = (1-\alpha)y[n-1] - \alpha x[n] \quad (2)$$

with $\alpha$ a configurable filter parameter. For the preliminary results, this parameter was set to 0.5. Once the signal is filtered, the value are communicated to the Bluetooth IC using a signed 24 bits integer format.

### 2.2.2 Communication Dedicated Software

In this section, the firmware of the BLE113 IC will be detailed. The scripting language provided by Silicon Labs, BGScript, was used to program this firmware. A custom GATT server was implemented with respect to the heart rate profile detailed in the Bluetooth 4 specification: the mandatory generic access profile, device information, heart rate and battery services were implemented. The heart-rate service was augmented with a customized heart rate variability characteristic. This characteristic is of length 5, and the SSDN, RMSSD, LF/HF ratio and normalized LF components ratio are encoded as single-byte unsigned integers. An additional service was implemented for the respiration along with another service dedicated to IoT-related information (i.e., information about the sensor non-functional states).

The BLE113 also implements device advertisement when the sensor is not connected and if a disconnection occurs according to the heart rate profile: the advertising interval is between 20 and 30 ms for the

first 30 seconds, and it is increased to be between 1 and 2.5 s for the next 30 seconds. If no device connect to the sensor after this advertising period, the sensor is put in a very low-energy deep sleep mode.

#### 2.2.3 IoT Dedicated Software

To enable our respiratory and cardiac activity sensor with IoT-based characteristics in order to include the object in wider IoT-based frameworks, the requirements are three-fold:

- The *data must be streamed in real time*, meaning as soon as a data is acquired, it must be transmitted.
- The sensor must be able to *provide information about its functional and non-functional state* in order to be able to build smart-scenarios based on the IoT-enabled devices.
- The sensor must be *remotely configurable* in order to be integrated to wider-scale auto-adaptation scenarios.

In order to fulfill this set of requirements, the sensor was modeled using a labeled transition system (LTS). LTSs are widely used models of computation (MoC) because of their relative simplicity and high expressiveness.

The LTS of our sensor is given in Figure **??**. The transitions between the states are either controllable (i.e., a remote tier can force the transition) or non-controllable (i.e., the sensor automatically determines its state from environmental measurements). As a convention, a transition written as "`a \ b`" means the transition is triggered on detection of internal event `a` or is remotely triggered using event `b`. When a transition is only labeled with a single event, it is assumed that this event is internal.

As displayed in Figure **??**, the sensor has 5 non-functional states:

- When turned on or after a reset operation, the sensor is in the **initialization** state. In this state, the AFE is configured with the default parameters and the BLE113 is software reset. This state automatically calls the normal operation state when the initialization process is over.
- The default state is the **normal** state. In this state, both ECG and respiration signal are acquired. The instantaneous heart-rate is sent in real time (i.e., the new value is transmitted as soon as it is available), the HRV parameters are computed every 5 minutes, and the respiration signal is packaged and transmitted every second.
- The **failsoft** state is an energy saving state. It is triggered either externally or when the battery level of the sensor reaches a low level (i.e., 20% in our case).
- When the sensor detects a disconnected lead, it is placed in the **unattached** state. In this state, a timer is launched, and the sensor is turned off if the timer overflows. If the sensor is reattached, it goes back to the normal operation state.
- The **stop** state denotes a very low-energy deep sleep mode. The sensor can be placed in this state at any time.

The BLE113 can generate "no connection" (abbreviated as "no_conn" in the LTS) events if the sensor does not receive any connection request during the advertising interval. This causes the sensor to go into the very low power stop state.

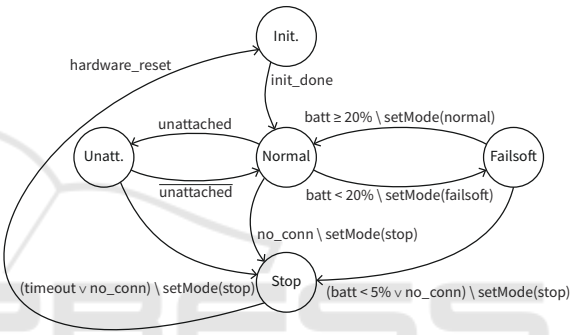


Figure 4.

Practically, this LTS is implemented on the ARM core of the PSoC5LP. Events are either generated internally or transmitted by the BLE113, and the sensor state is exposed using a custom service.

### 2.3 Gateway Software and IoT-Based Framework

Android phones were chosen as the main gateways to our sensor. This choice was motivated principally because phones can be carried by the subjects, resulting in a mobile gateway with perpetual connection to the Internet. Consequently, an Android application was developed to connect to the sensor, but also to plot the data, store it locally on the phone or transmit them over the Internet. The application is based on the nRF Toolbox open-source application[1] developed by Nordic Semiconductor (Oslo, Norway), and screenshots of the application are given in Figure 5.

Because data is collected in real time and sensor configuration can be triggered at any moment, a publish/subscribe type protocol was chosen. Practically,

[1] https://github.com/NordicSemiconductor/Android-nRF-Toolbox

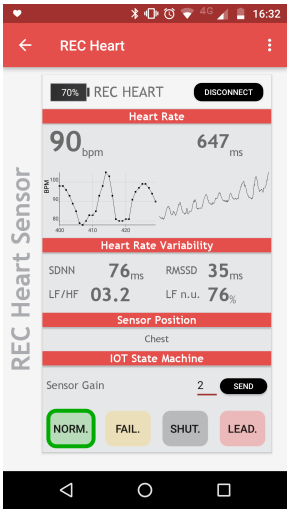


Figure 5: Companion Android application.

the Eclipse Paho MQTT client was integrated in the application. MQTT is a lightweight publish/subscribe messaging Internet-based protocol. It was designed to be used in memory and bandwidth constrained devices. This protocol is built around the notion of topics. A topic is an URI-like string used to describe transiting data. In the MQTT terminology, a *publisher* sends data in a topic. If a *subscriber* subscribes to the same topic, it will receive the data instantaneously. Formally, all data is sent through a central *broker* that can be seen as a hub distributing data between the relevant publishers and subscribers. This publish/subscribe mechanism thus implements real-time data streaming over the Internet, and enables connection to various external Web services or other connected devices.

# 3 RESULTS

## 3.1 Power Consumption Characterization

In this section, a comprehensive evaluation of the sensor power consumption with respect to connection parameters and non-functional IoT-state defined in Figure 4 is performed.

Current consumption measurements were performed using a Keithley 2400 sourcemeter (Beaverton, OR, USA). The first characterization to be performed was a static power consumption evaluation of the normal, failsoft, and stop states. The initial state was not measured because it is only a transitional state with a short duration, and the unattached state was not measured because the sensor is in the same hardware configuration than in the normal state, resulting in equal power consumption. This static characterization was performed using default Android 7.0 BLE connection parameters (i.e., connection interval of 48.75 ms, timeout of 20 s and latency of 0). The consumption results are given in Table 2. With a power consumption of 10.53 mW in the normal state, the battery life of the sensor if of about 75 hours using a 300 mAh battery. This battery life is extended to about 85 hours if the failsoft mode is used. In the stop mode, the sensor can last more than two months on a fully charged battery.

Table 2: Static power characterization of IoT states.

| IoT state | Power consumption (mW) |
|---|---|
| Normal | 10.53 |
| Failsoft | 9.18 |
| Stop | 0.505 |

In order to further optimize power consumption of the sensor, the influence of the BLE connection parameters were also studied. There are three BLE connection parameters: interval, latency and timeout. The connection interval designates the period between two master's requests to the slave, while the latency defines the number of connection intervals that can be ignored safely by the slave. Finally, the connection timeout designates the period after which the BLE master will consider that the connection with the slave is lost. It is only after the timeout period that the BLE master can attempt with reconnection. For the sensor, we fixed both the connection interval and connection timeout, and the impact of the latency was studied on the overall power consumption. The results of this characterization are given in Figure 6, and the consumption of both the normal IoT state and the failsoft IoT state are plotted against the latency for various connection interval and connection timeout. For all states and connection interval and timeout parameters, and increase in the latency results in decreasing overall power consumption, with a stronger decrease for smaller latency values. It is worth noting that for a latency of 8, connection instability was observed. In order to enable smaller power consumption, while keeping acceptable connectivity quality, the sensor requests a latency of 2 when a new connection is established. However, masters (such as Android phones) can reject connection parameters update and force a new set of less constrained connection parameters (i.e., smaller connection intervals, zero latency and smaller connection timeout), causing an increase in the overall power consumption. This problem was solved with a slight oversizing the battery capacity in order to always achieve at least 48 hours of battery life.

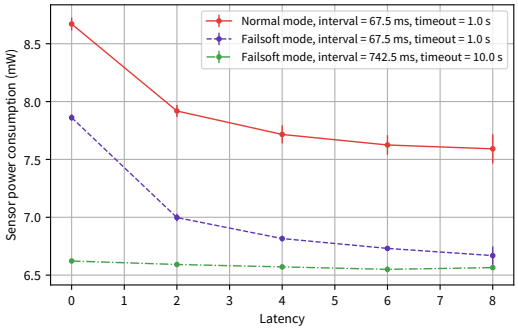


Figure 6: Characterization of the BLE connection latency parameter effect on the overall power consumption.

## 3.2 Data Acquisition

In this section, various data acquisition are presented. This first experiment to be performed was the validation of RR-interval acquisition using synthetic ECG signals generated using an Agilent 33220A (Santa Clara, CA, USA) arbitrary waveform generator. The objective of this test is twofold: it validates the computation of RR-interval and the reliability of the BLE connection. In order to simulate heart rate variability, triangular frequency modulation was applied to the synthetic ECG signal:

$$\begin{aligned} \text{base frequency} &= 1.25 \text{ Hz} \\ \text{frequency deviation} &= 200 \text{ mHz} \end{aligned} \tag{3}$$

which theoretically results in RR intervals ranging between:

$$\begin{aligned} RR_{\text{int}} &< \frac{1000}{1.25-0.2} \approx 952.4 \text{ ms} \\ \text{and, } RR_{\text{int}} &> \frac{1000}{1.25+0.2} \approx 689.7 \text{ ms} \end{aligned} \tag{4}$$

The sensor was then connected to a Raspberry Pi used as a BLE data logger to record RR-intervals and HRV parameters, and an excerpt of the collected RR interval values is given in Figure 7. The experiment was performed during 1 day, 17 hours and 9 minutes. A total of 185153 were logged. Data was analyzed for records violating the theoretical limits (with a tolerance of 1% over the limits), and no violations were found.

The next experiment was data acquisition during short respiratory exercises. During this exercise, a young healthy patient was asked to perform a series of forced inspiration and expiration during 1 minute in order to trigger sinus arrhythmia. Results from this experiment are given in Figure 8, where both the instantaneous heart rate and the normalized respiratory waveform are plotted. This figure clearly illustrates sinus arrhythmia, with increasing heart rate during

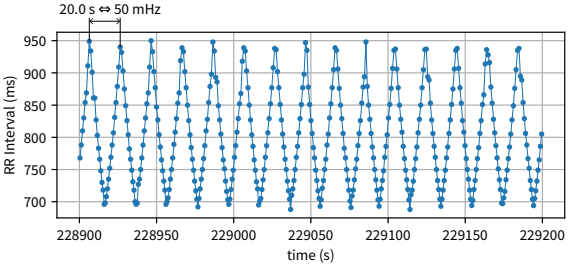


Figure 7: RR interval determined from synthetic ECG signal.

inspiration because of a decreasing vagal tone and decreasing during expiration.

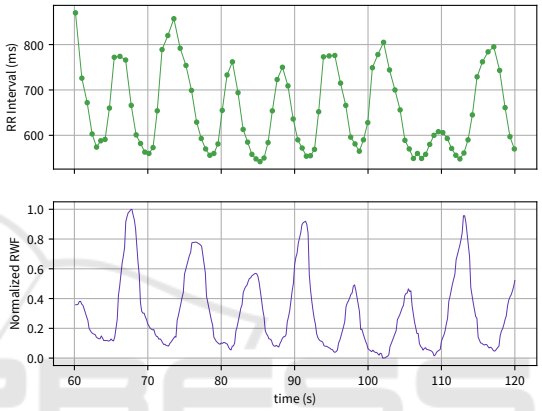


Figure 8: RR-Interval and respiratory waveform during controlled respiratory exercise.

The final experiment consisted on a short-term ambulatory testing of the sensor. For this experiment, a patient was asked to wear the sensor during one hour, while performing normal daily activities. Cardiorespiratory data was recorded using the companion Android application, and results from this experiment are given in Figures 9 and 10. Figure 9 displays both the instantaneous RR interval and normalized respiration signals. No measurement artifact were observed for both the signals. ECG artifacts, resulting in RR interval artifacts, are typically caused by electrical muscular activity interfering with ECG signals. Such adverse effects were minimized by placing on the lower part of the rib cage. Indeed, this location features minimal muscle thickness, thus reducing interactions between ECG signal and electrical muscular activity. It is worth noting that the respiration signal features a slowly evolving component. This is because the respiratory activity is in fact an impedance measurement, and because the impedance of the electrode-skin interface can slowly evolve over time because of various factors (such as humidity, the presence of sweat, etc.). This can be corrected by applying a high-pass filter during signal post-processing.

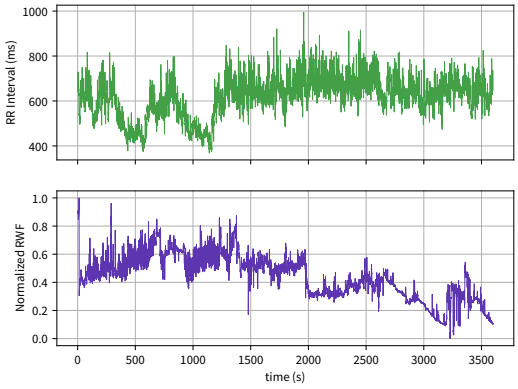


Figure 9: Real-life RR-Interval and respiratory waveform.

Figure 10 displays the 4 heart rate variability parameters plotted as a function of time. These HRV parameters correspond to the HR measurements exhibited in Figure 9, and fall within the typical ranges defined by the literature (Nunan et al., 2010).

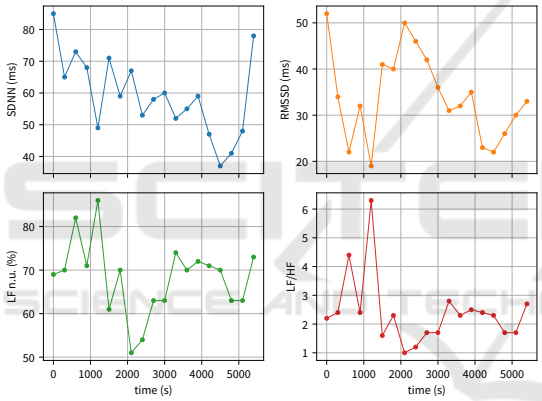


Figure 10: Real-life HRV parameters.

The preliminary results presented herein-above proves that our wearable sensor provides high quality data. The next experiment will deal with the integration of our wearable sensor in wider-scale IoT-based healthcare framework.

### 3.3 Integration to an IoT-Based Framework

As specified in Section 2, the integration of our wearable sensor to wider-scale healthcare frameworks occurs through the Android companion application. Indeed, upon sensor connection, the application attempts to connect to a local MQTT broker. If the connection is successful, the application will publish heart rate and HRV values as soon as they are available on two topics:

- `interface/hr`
- `interface/hrv`

As a result, cardiac parameters are streamed in real time using these two topics, and this is the basis to build wider-scale healthcare framework. As a proof of concept, a monitoring Web-based graphical user interface was implemented. It simulates the kind of GUI that can be made available to physicians in order to have real time health information on their patients. A sample screenshot of the Web-based GUI is given in Figure 11.

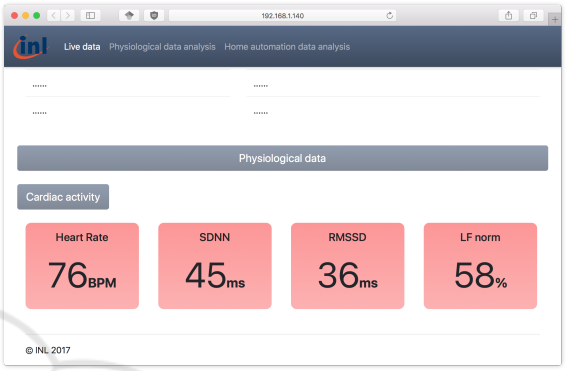


Figure 11: Web application visual.

## 4 DISCUSSION

In this paper, we introduced a wearable cardiorespiratory sensor that can be easily integrated to wider-scale healthcare framework. This sensor satisfies crucial healthcare-related requirements such as data realiability, remote configuration capabilities or scalability. Wearable healthcare and the Internet-of-Things have similar objectives: the use of a mass of connected objects (which also are worn by patients in the context of wearable healthcare) that monitor physical parameters in order to trigger medical advice or intervention based on data analysis. For instance, our wearable sensor can be integrated in a living-lab, where the living environment of the patient is continually monitored. This integration relies on the use of widely adopted technologies such as BLE, but also on Internet-based technologies such as MQTT in order to enable wide-scale connectivity. Internet-based connectivity implies that our wearable sensor is able to connected to Internet healthcare services, which can perform advanced data analysis and detect potential health crisis of the patient and trigger urgent medical response.

Wearable healthcare have a strong potential on the improvement of the patients' quality of life and quality of care. Indeed, the wearable nature of devices enable patients to be continuously remotely monitored. Combined with recent advances in home-automation,

wearable healthcare will drastically improve in-home care for a variety of patients. Collected data processed using big-data techniques or advanced signal processing could also have great predictive values for the evolution of chronic diseases and could be used to provide better and earlier care for patients.

However, the personal nature of collected health data mandates strong security mechanism, which were not explored in our contribution. Indeed, at the moment our system only features basic data encryption in compliance with the BLE standard, and the MQTT-based solution does not use any security mechanism. Security of our overall system needs to be improved, more particularly in terms of access control (i.e., the patients of physicians must be able to know and control who accesses their medical data) and identity management, and recently developed decentralized blockchain-based solutions (Zhu et al., 2017) can be explored in order to provide comprehensive werable healthcare system security.

## 5 CONCLUSION

In this paper, we presented a multiparametric, cardiorespiratory wearable sensor. In order to answer healthcare requirements, more particularly in terms of the ability to integrate wearable sensors into wider-scale frameworks, we considered an IoT-based approach. Indeed, we equipped our sensor with remote configuration capabilities while preserving quality-of-data and real-time streaming capabilities, which are key requirements of wearable healthcare systems. This sensor was implemented using carefully selected hardware, and it was comprehensively characterized in terms of energy consumption, which is another major concern of wearable healthcare devices. Indeed, because battery charging usually implies the sensor is not collecting physiological data, potentially relevant data can be lost, and the charging time to battery life ration must thus be as big as possible. The data collection capabilities of our sensor were also extensively tested on both synthetic ECG signals and in real-life ambulatory conditions. Successful testing and integration to Internet-based framework proved that our sensor can be used in a wide-scale wearable healthcare framework.

## ACKNOWLEDGMENT

The authors would like to thank the COOPERA funding program of Région Auvergne Rhône-Alpes for their generous financial support.

## REFERENCES

Altini, M., Polito, S., Penders, J., Kim, H., Van Helleputte, N., Kim, S., and Yazicioglu, F. (2011). An ECG patch combining a customized ultra-low-power ECG SoC with bluetooth low energy for long term ambulatory monitoring. In *Proceedings of the 2nd Conference on Wireless Health*, pages 15:1–15:2, New York, NY, USA. ACM.

Fernandez, F. and Pallis, G. C. (2014). Opportunities and challenges of the internet of things for healthcare: Systems engineering perspective. In *Proceedings of the EAI International Conference on Wireless Mobile Communication and Healthcare*, pages 263–266.

Gubbi, J., Buyya, R., Marusic, S., and Palaniswami, M. (2013). Internet of things (IoT): A vision, architectural elements, and future directions. *Future Generation Computer Systems*, 29(7):1645 – 1660.

Harris III, A. F., Khanna, V., Tuncay, G., Want, R., and Kravets, R. (2016). Bluetooth low energy in dense IoT environments. *IEEE Communications Magazine*, 54(12):30–36.

Izumi, S., Yamashita, K., Nakano, M., Kawaguchi, H., Kimura, H., Marumoto, K., Fuchikami, T., Fujimori, Y., Nakajima, H., Shiga, T., and Yoshimoto, M. (2015). A wearable healthcare system with a 13.7 $\mu$A noise tolerant ecg processor. *IEEE Transactions on Biomedical Circuits and Systems*, 9(5):733–742.

Khayatzadeh, M., Zhang, X., Tan, J., Liew, W. S., and Lian, Y. (2013). A 0.7-V 17.4-$\mu$W 3-lead wireless ECG SoC. *IEEE Transactions on Biomedical Circuits and Systems*, 7(5):583–592.

Lomb, N. R. (1976). Least-squares frequency analysis of unequally spaced data. *Astrophysics and Space Science*, 39(2):447–462.

Magno, M., Spagnol, C., Benini, L., and Popovici, E. (2014). A low power wireless node for contact and contactless heart monitoring. *Microelectronics Journal*, 45(12):1656–1664.

Massot, B., Noury, N., Gehin, C., and McAdams, E. (2013). On designing an ubiquitous sensor network for health monitoring. In *Proceedings of the International Conference on e-Health Networking, Applications and Services*, pages 310–314.

Massot, B., Risset, T., Michelet, G., and McAdams, E. (2015). A wireless, low-power, smart sensor of cardiac activity for clinical remote monitoring. In *Proceedings of the International Conference on E-health Networking, Application Services*, pages 488–494.

Massot, B., Risset, T., Michelet, G., and McAdams, E. (2016). Mixed hardware and software embedded signal processing methods for in-situ analysis of cardiac activity. In *Proceedings of the 9th International Joint Conference on Biomedical Engineering Systems and Technologies*, pages 303–310.

Nunan, D., Sandercock, G. R., and Brodie, D. A. (2010). A quantitative systematic review of normal values for short-term heart rate variability in healthy adults. *Pacing and Clinical Electrophysiology*, 33(11):1407–1417.

Press, W. H. and Rybicki, G. B. (1989). Fast algorithm for spectral analysis of unevenly sampled data. *The Astrophysical Journal*, 338:277–280.

Schäfer, A. and Vagedes, J. (2013). How accurate is pulse rate variability as an estimate of heart rate variability?: A review on studies comparing photoplethysmographic technology with an electrocardiogram. *International Journal of Cardiology*, 166(1):15 – 29.

Task Force of the European Society of Cardiology the North American Society of Pacing Electrophysiology (1996). Heart rate variability: Standards of measurement, physiological interpretation, and clinical use. *Circulation*, 93(5):1043–1065.

Tuominen, J., Lehtonen, E., Tadi, M. J., Koskinen, J., Pnkl, M., and Koivisto, T. (2017). A miniaturized low power biomedical sensor node for clinical research and long term monitoring of cardiovascular signals. In *Proceedings of the International Symposium on Circuits and Systems*, pages 1–4.

Van Hoof, C. and Penders, J. (2013). Addressing the healthcare cost dilemma by managing health instead of managing illness: An opportunity for wearable wireless sensors. In *Proceedings of the Conference on Design, Automation and Test in Europe*, pages 1537–1539. EDA Consortium.

Winter, B. B. and Webster, J. G. (1983). Driven-right-leg circuit design. *IEEE Transactions on Biomedical Engineering*, 30(1):62–66.

Zhao, L., Reisman, S., and Findley, T. (1994). Respiration derived from the electrocardiogram during heart rate variability studies. In *Proceedings of 16th International Conference of the IEEE Engineering in Medicine and Biology Society*, pages 123–124.

Zhu, X., Badr, Y., Pacheco, J., and Hariri, S. (2017). Autonomic identity framework for the internet of things. In *Proceedings of the International Conference on Cloud and Autonomic Computing*, pages 69–79.